FFI RAPPORT

GAP TEST EXPERIMENTS USED TO STUDY THE SENSITIVITY OF GRANULAR EXPLOSIVES

Eriksen Svein W, Moxnes John F, Strømgård Monica

FFI/RAPPORT-2004/01882

FFI-V/860/01

GAP TEST EXPERIMENTS USED TO STUDY THE SENSITIVITY OF GRANULAR EXPLOSIVES

Eriksen Svein W, Moxnes John F, Strømgård Monica

FFI/RAPPORT-2004/01882

FORSVARETS FORSKNINGSINSTITUTT
Norwegian Defence Research Establishment
P O Box 25, NO-2027 Kjeller, Norway

FORSVARETS FORSKNINGSINSTITUTT (FFI)
Norwegian Defence Research Establishment

P O BOX 25
N0-2027 KJELLER, NORWAY

UNCLASSIFIED

SECURITY CLASSIFICATION OF THIS PAGE
(when data entered)

REPORT DOCUMENTATION PAGE

1) PUBL/REPORT NUMBER	2) SECURITY CLASSIFICATION	3) NUMBER OF PAGES
FFI/RAPPORT-2004/01882	UNCLASSIFIED	29
1a) PROJECT REFERENCE	**2a) DECLASSIFICATION/DOWNGRADING SCHEDULE**	
FFI-V/860/01	-	

4) TITLE

GAP TEST EXPERIMENTS USED TO STUDY THE SENSITIVITY OF GRANULAR EXPLOSIVES

5) NAMES OF AUTHOR(S) IN FULL (surname first)

Eriksen Svein W, Moxnes John F, Strømgård Monica

6) DISTRIBUTION STATEMENT

Approved for public release. Distribution unlimited. (Offentlig tilgjengelig)

7) INDEXING TERMS

IN ENGLISH:	IN NORWEGIAN:
a) explosives	a) eksplosiver
b) sensitivity	b) følsomhet
c) Autodyn	c) Autodyn
d) granular	d) granulære
e) deflagration	e) deflagrasjon

THESAURUS REFERENCE:

8) ABSTRACT

Explosives are widely used in medium to large calibre projectiles to increase the damage on a target. The ammunition produced by Nammo Raufoss, has superb qualities concerning penetration and fragmentation in a target. Enhanced fragmentation effect is achieved though a deflagration of a press filled granular explosive, which gives larger and more appropriate fragments compared to ordinary ammunition, which detonates. To control the time for the delayed action of the explosive/ fragments due to impact, the sensitivity of the explosive is important to control both experimentally and numerically.

In this article we present a small-scale gap test experiment that is developed to study the sensitivity of the explosives. The experimental set up is rather easy and cheap. We show that the sensitivity of the different explosives is very different. We also show that the shock sensitivity is uncorrelated with standard Bam fall hammer and friction tests.

9) DATE	AUTHORIZED BY	POSITION
	This page only	
11 Februar 2004	Bjarne Haugstad	Director of Research

ISBN 82-464-0917-4

UNCLASSIFIED

SECURITY CLASSIFICATION OF THIS PAGE
(when data entered)

CONTENTS

Page

GAP TEST EXPERIMENTS USED TO STUDY THE SENSITIVITY OF GRANULAR EXPLOSIVES

1 INTRODUCTION

Explosives are widely used in projectiles to increase the damage of a target. The MP ammunition produced by Nammo Raufoss, has superb qualities concerning penetration and fragmentation in a target. Enhanced fragmentation effect against weak targets is achieved though a deflagration of a press filled granular explosive, which gives larger and more appropriate fragments compared to ordinary ammunition, which detonates. During use against hard targets the ammunition most likely detonates. To control the time of the delayed action of the explosive/ fragments due to impact, the sensitivity of the explosive is important to control both experimentally and numerically. One special experimental design is the gap test.

These gap test experiments are well known and used to study the detonation threshold for explosives. The ordinary gap test consists of a cylinder of a well-known explosive (donor). This cylinder detonates along the axis of symmetry. Another explosive charge in a tube of steel (acceptor) is placed some gap distance from the detonator along the axis of symmetry. The spacing between the two charges is varied along the axis of symmetry to find the threshold for detonation of the acceptor. The threshold is typically found by visually observing the deformation pattern of the steel tube surrounding the acceptor charge. Typically the spacing between the donor and the acceptor is filled with plastic cards or water.

The ignition threshold for explosives is dependent of many factors. The most important ones are the type of explosive, the grain size, the density and the amount of binder. To study the ignition mechanisms more fundamentally, it is important also model the compacting behaviour during compression. We believe that this behaviour is most easily studied by doing computer simulations. Also the water or the plastic cards that ordinary constitutes the gap between the donor and the acceptor complicates the computer simulations since also the water or the plastic card have to be modelled. It is therefore of interest to model the gap test more directly where only vacuum separates the donor from the acceptor. Also be believe that the typical scale of the design used during gap test is too large and therefore not cost effective. Thus the reason for our somewhat uncommon design is all-together:

- A need to simulate the gap test by computer simulations in order to understand the physical mechanisms better
- The simulation of standard gap tests becomes un necessary complicated due to the necessary modelling of water and plastic in the gap between the donor and the acceptor.
- The size of the standard gap test is too large and costly.

During impact on explosives we can fundamentally separate between four different thresholds

- The threshold for significant hot spot ignition due to localized hot areas
- The threshold for ignition due to adiabatic compression
- The threshold for run up to detonation
- The threshold for detonation

During hot spot ignition the adiabatic compression of the explosive is too low to reach a global temperature near the decomposition temperature of the explosive. But explosive still ignites due to localized hot areas. These hot spots are due to localized hot bubbles due to compressed air pockets or due hot areas due to friction between sliding surfaces in the explosive. During hot-spot ignition a granulate typically ignites and burn from the surface of the particles. This burning can fade away due to decreased pressure or it can build up to a detonation. A detonation is not reached unless the confinement of the ignited areas is large.

Ignition by adiabatic compression is typically reached for high pressures above 2 GPa. The temperature due to the compression is at the decomposition temperature of the explosive. The decomposition of is then complete.

During run up to detonation the gas pressure becomes larger than the initial ignition pressure. The gas pressure is initially still below the detonation pressure due to low density of the compressed solid material. But the gas pressure compress and ignites new material ahead. The corresponding gas pressure usually becomes higher than the initial pressure, which compressed the solid material. Finally the pressure during compression of the non-decomposed material becomes the same pressure as the gas pressure. The escalating then stops, and a full detonation is reached. The self-sustained detonation quickly run through the explosive charge with a velocity around 7000 -8000m/s.

Although our main concept is very equal to the well-known gap test, our focus is quite different since MP ammunition deflagrates during use on light targets and probably detonates during use on hard targets. We therefore use the gap test to study both the threshold for significant hot-spot ignition and the threshold for detonation. Although our main focus in this report is to study sensitivity near the threshold for detonation, i.e. ignition stimulus during use of the ammunition against hard targets. The sensitivity of different explosives will be compared.

Our first problem was to seek a gap between the detonator and the acceptor such that the ignition pressure on the acceptor is equal to the pressure on the ignition pressure on the explosive in the ammunition when the ammunition hits hard targets. This critical gap distance can be achieved in two different ways. The first is based on computer simulations of the projectile during impact and computer simulations of the gap test. First we numerically find the pressure on the explosive during impact in a target. Thereafter the gap test is simulated to find the gap necessary to achieve the same pressure on the acceptor. The second way is purely experimentally, i.e. the necessary gap distance is found by running different gap tests experiments in the laboratory.

After finding the critical gap test, the sensitivity of the different explosives is studied by studying the deformation pattern of the steel tube for this given gap size. Three different HMX based explosives are studied in this article. The difference between the explosives is the grain size, the density and the coating. We find large differences in the shock sensitivity of the explosives near the detonation threshold. The sensitivity is positive correlated with the grain size. Any difference in the sensitivity due to changing densities is not observed. Also the sensitivity is shown to be uncorrelated with sensitivity during Bam fall hammer and Bam friction tests. Thus the shock sensitivity cannot in general be found by using results from these standard tests.

Section 2 presents the experimental set-up. Section 3 presents the computer simulations.
Section 4 presents the experimental results. Finally section 5 concludes.

2 EXPERIMENTAL SET-UP

Figure 2.1 show a picture of the experimental set- up.

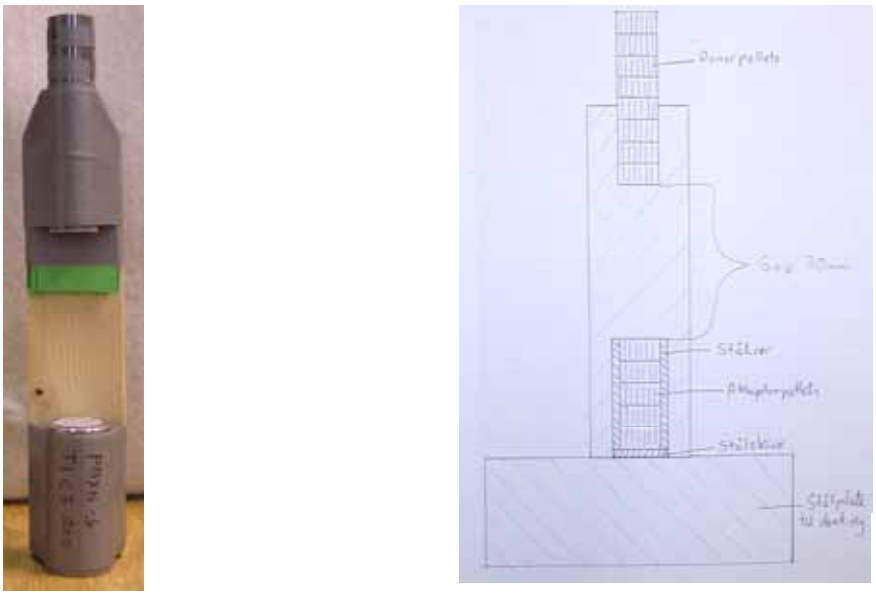

Figure 2.1: The experimental set-up

The donor charge consists of 8 pellets of PBXN5-T2-C1 of density 1.79 g/cm^3 pressed and thereafter glued together along a line. Thereby giving a total axial length of approximately 8 cm. The diameter of the pellets is 17.14 mm. The mass of each pellet is approximately 4 grams. The height is approximately 9.7 mm.

The acceptor charge consist of 5 pellets of explosive placed together into a cylindrical tube of steel with thickness of 4mm, outer diameter 25 mm and length 50 mm. The gap between the donor and acceptor is 70 mm. The height of the each pellets is approximately 9.7 mm but is somewhat varying due to different densities. This is accounted for when defining the gap size. Three different explosives are used and two different densities are used. Also a disk of thickness 4 mm is supporting the acceptor charge. The total configuration is then placed on a ticker supporting steel plate (not shown in the figure). Thereby the dent in this supporting plate can be observed and recorded. The material properties and the geometrical dimensions of the acceptor is given in appendix A.

3 NUMERICAL RESULTS FROM AUTODYN

In order to find the critical gap size and to study the fragmentation pattern Autodyn [1] simulations were used.

Figure 3.1a shows the set up for simulation of 12.7mm MP ammunition hitting a 22mm armour steel plate at 900 m/s. The yield stress of the steel plate is 1.1 GPa. Figure 3.1b shows a typical deformation pattern of the 12.7 MP ammunition when hitting the target. Figure 3.1c shows the pressure when hitting the target. Observe that the pressure in the explosive is close to 2 GPa. During use the ammunition ignites. Thus we find that during use the critical ignition pressure is close to 2 GPa.

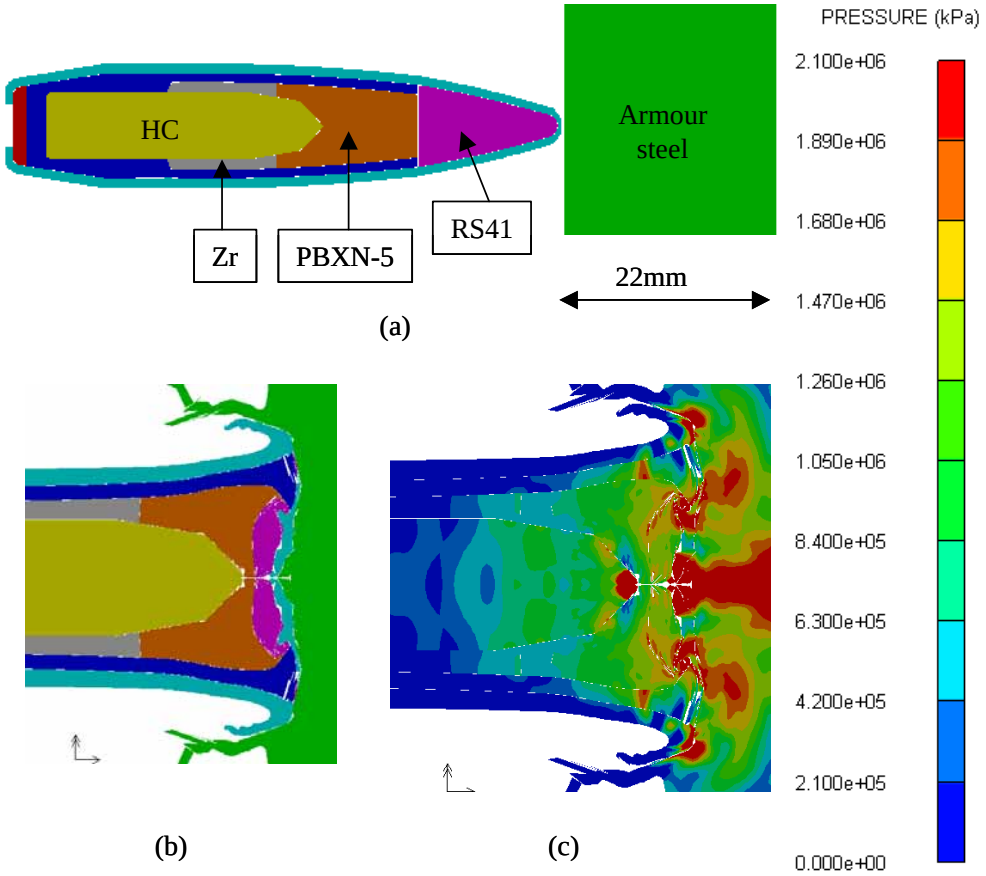

Figure 3.1. (a) Set up for simulation of the 12.7mm MP hitting 22mm armour steel, (b) Typical deformation pattern and (c) pressure just before the tungsten carbide hardcore hits the target.

The geometrical set up for the gap test simulation is shown in figure 3.2. The gap size is varied. The powder model adjusted for shock is used as the acceptor. The pressure in the donor is 37 GPa. The input parameters for the simulations are given in appendix A for the donor (PBX-9404-3) and in appendix B for the acceptor. Appendix c shows the material parameters for the steel. Figure 3.3 shows the pressure variation in the front of the acceptor as a function of the distance to the donor (the gap size). This pressure should then correspond with the ignition pressure. We observe that at a distance of 70 mm the pressure is close to 2 GPa. Thereby in agreement with ignition pressure for the firing simulations in figure 3.1c. The

numerical simulations thus suggest that a gap size of approximately 70 mm should be used for the experimental se-up to mimic the firing experiments.

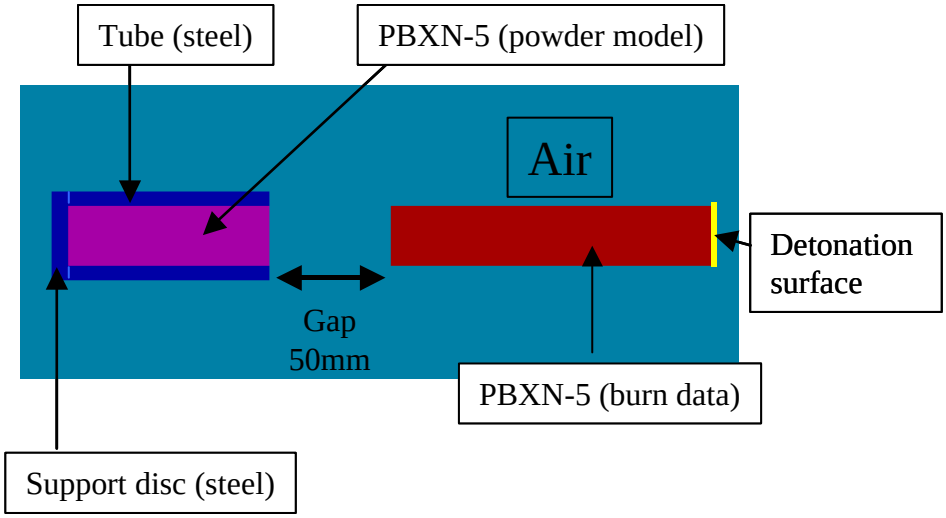

Figure 3.2. The geometrical set up for the gap test simulations. The steel tube is 50mm in length, inner diameter is 17.3mm and outer diameter is 25.3mm (wall thickness is 4mm). The disc is 4mm in thickness and 25.3mm in diameter.

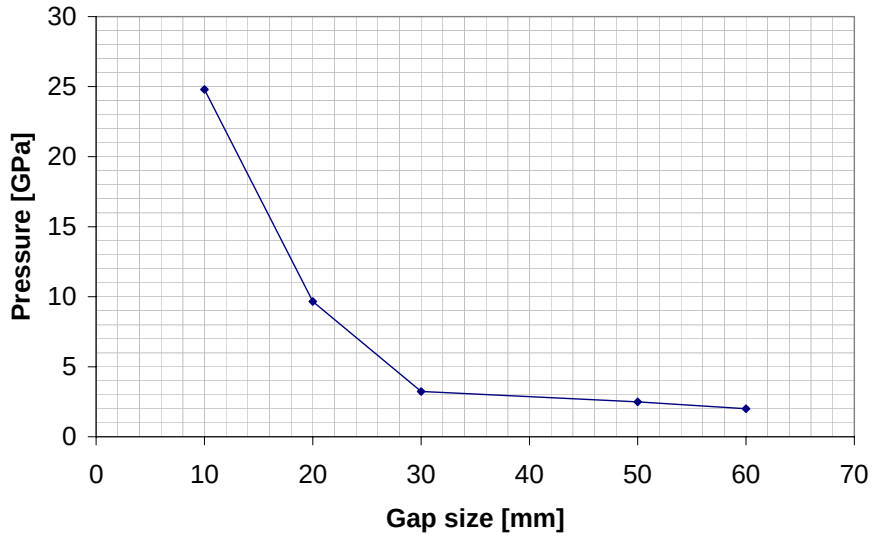

Figure 3.3. The pressure in the acceptor as a function of the distance to the detonator (the gap size)

Figure 3.4 shows the set up for simulation of the deformation of the steel tube and steel disc when detonating the acceptor explosive. The material data for the explosive in these simulations is given in appendix A (PBX-9502). The rear part of the supporting steel plate below the steel disc was not allowed to move axially. In figure 3.5 the deformation of the steel tube and disc is shown. (a) Shows the deformation (fragmentation) for a normal detonation where the detonation velocity is 7700 m/s and (b) shows the deformation for an abnormal

detonation where the detonation velocity is only 1000 m/s. For the normal detonation the dent in the supporting plate was 2.75 mm. For a full detonation the experimental results show 3.85 mm. This disagreement is probably related to the incorrect input material parameters for the steel-supporting plate. The hardness of the supporting plate is between 135-170HV. This correspond to a yield limit between 4 10^8 and 5 10^8 Pa. This value is somewhat lower than the 6.5 10^8 used for the simulations. The indentation depth scales roughly as the yield strength of the supporting plate. Thus the simulated value of 2.75 mm could be scaled up to 3.58-4.47mm.

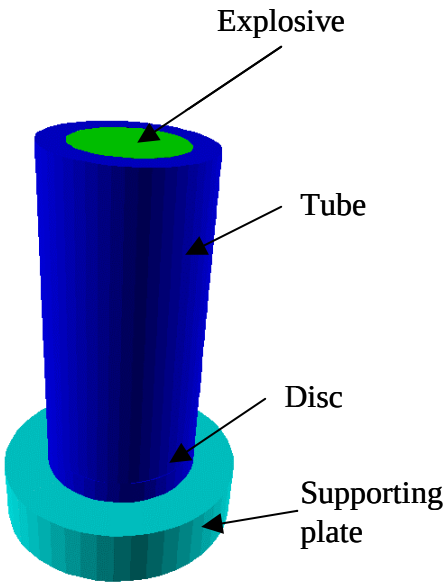

Figure 3.4. Set up for the simulations of the deformation of the steel tube and steel disc when detonating the acceptor explosive.

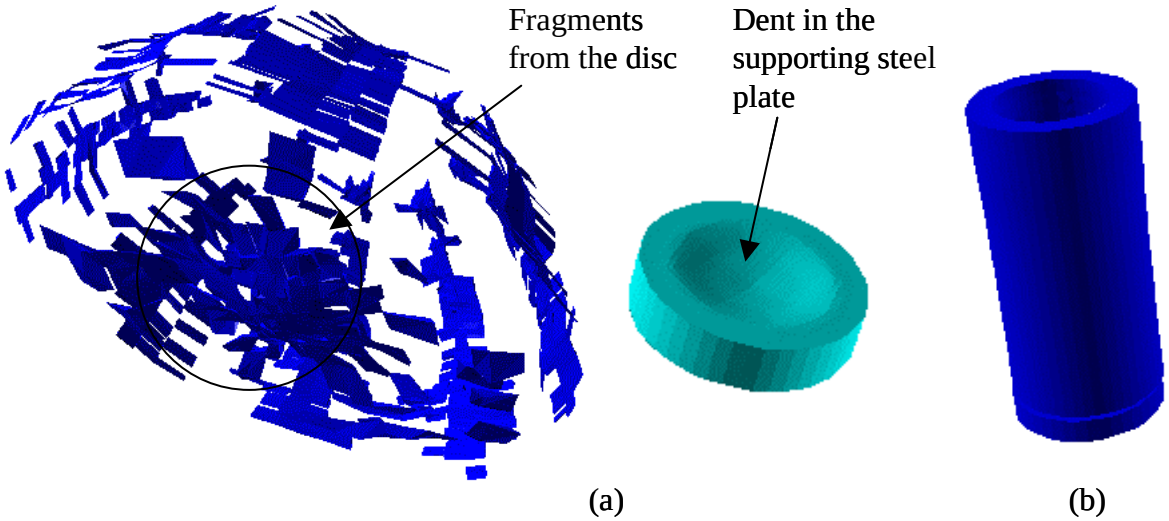

Figure 3.5. (a) The deformation patterns of the pipe and disc and the dent in the supporting plate for a normal detonation. (b) The deformation pattern for an abnormal detonation.

For the abnormal detonation the dents in the supporting plate was insignificant. This is also what we find experimentally for the situations where the cylinder was marginally deformed.

The conclusion from the simulations then are: i) a gap size of approximately 70 mm should be used for the experimental set up to mimic the ignition pressure of 2 GPa during use of the ammunition against hard targets, ii) during a full detonation the number of fragmentations is large, and much larger than observed during use of the ammunition for light targets. The dent in the supporting plate should be approximately 2.75 mm, iii) during abnormal detonation the dent in the supporting plate and the deformation of the cylindrical tube should be insignificant.

4 THE EXPERIMENTAL RESULTS

Three different explosives where tested. Table 4.1 show the different types

Name	Composition	Grain structure	Granular structure	Maximum density	Comments on grain structure
H764	98% HMX,1%Ca resinate,1%Grapite	100%USS18 27%USS 27	-None	1.89g/cm^3	Coarse
PBXN-5,T2,C1	95%HMX,5%Viton	75% K1, 25% K5	C1	1.90g/cm^3	Medium
PBXN-5,T1,C3	95%HMX,5%Viton	100% K5	C3	1.90g/cm^3	Fine

Class	Min	Max	USS Sieve
K1	90%USS 50,50%USS100 20%USS200,13%USS325	-	
K5	98%USS325 (0,045mm)		
C1	98% USS4 0% USS40	100% USS4 5% USS40	
C2	100% USS4 50% USS20 0% USS40	100% USS4 100% USS20 5% USS40	
C3	100%USS4 100%USS20 0%USS50	100%USS4 100%USS20 5% USS50	

Table 4.1: The different acceptor explosives used for the gap test

The donor explosive was always of type PBXN-5 T2-C1, with a density of 1.787 g/cm^3.

Calibration

Using a zero gap size for the acceptor PBXN-5 T2-C1 set up our first calibrating experiment. Thereby a full detonation was achieved. The fragments were recorded and the dent in the supporting plate was observed. Also other shots with gap sizes up 50 mm were examined. The fragmentation pattern was roughly the same. Thus indicating a full detonation. The typical

fragments are seen in figure 4.1. Table 4.2 shows the experimental results together with the simulation results.

	Acceptor	Density	Gap size	Fragments	Dent
Experimentally	PBXN-5 T2-C1	1.79g/cm^3	0.0	Many	3.82-3.90mm
Simulations	PBX-9502	1.90g/m^3	0.0 0.0	Many	2.75mm

Table 4.2: Results during full detonation

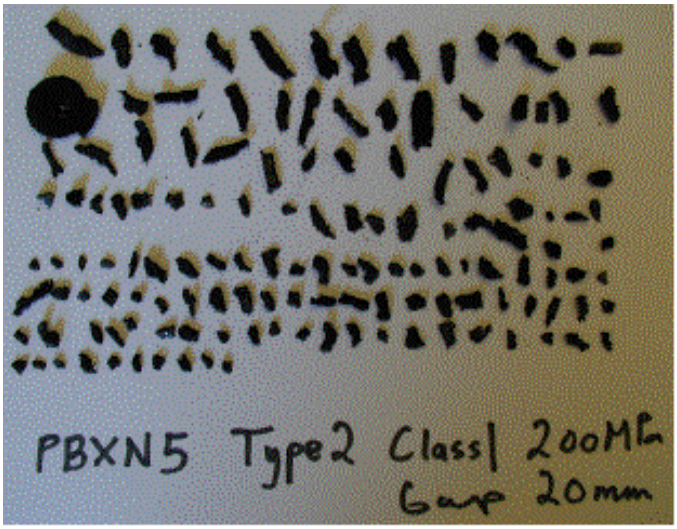

Figure 4.1. Fragmentation during full detonation.

For a gap size of 70 cm a clear difference in the fragmentation pattern for the different explosives was seen. According to figure 3.3 this gives a pressure on the acceptor equal to 2 GPa. This pressure is in good agreement with the pressure on the explosive during use of the ammunition against hard targets.

H764

Figure 4.2 shows the fragments when the gap size is 70 cm. The fragments and the dent in the supporting plate indicate that we are close to a detonation. We have also varied the density of the pellets by varying the pressure between to 200 and 300 MPa. No difference between those two cases is observed.

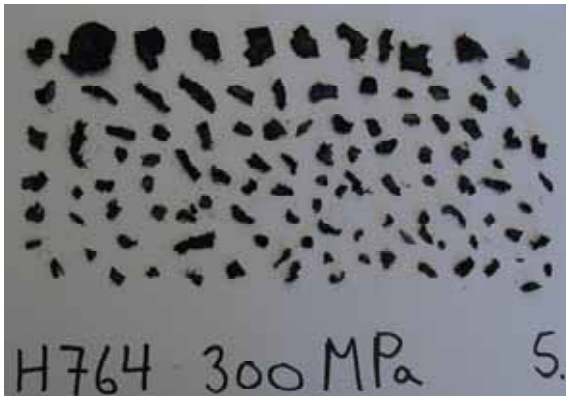

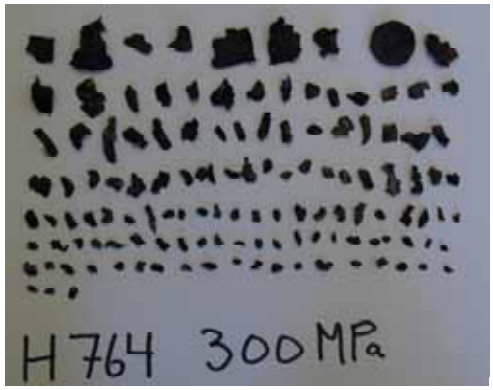

Figure 4.2: Fragments for H764, gap size 70mm.

Acceptor	Density	Pressure	Fragments %	Dent	Shots
H764	1.745g/cm^3	200MPa	Many, 74%	3.72-3.85-3.90mm	5
H764	1.767g/cm^3	300MPa	Many, 78%	2.84-3.43-3.92mm	5

Table 4.3: H764, gap size 70 mm.

PBXN-5-T2-C1

Figure 4.4: PBXN5-T2-C1, gap size 70mm

Figure 4.4 shows the fragments when using PBXN5-T2-C1. The fragments are much larger than for H764. The 200 MPa case up in the right corner is believed to be atypical. Due to limited amount of explosive we were not able to do more test of the 200 MPa charges, but there is probably some difference between the 200 and 300 MPa situation. By examining the fragments they suggest that the pressure in the ignition front of the acceptor is decaying along the tube.

Acceptor	Density	Pressure	Fragments %	Dent	Shots
PBXN-5 T2-C1	1.77g/cm^3	200MPa	Many, 85%	0.04-2.83mm	4 (2)*
PBXN-5 T2-C1	1.79g/cm^3	300MPa	Many, 80%	0.06-0.13-0.23mm	5

Table 4.4:PBXN5-T2-C1, the dent was found from only two shots.*

PBXN-5-T1-C3

Figure 4.5 shows the fragments. The deformation of the steel tube is small. The dent is not visible. No clear difference between the 200 and 300 MPa case is observed. The tube showed the smallest diameter at the rear end (close to the disk). This suggests that the pressure is decaying along the tube. Thus we expect that the ignition will dismiss for an infinite long tube.

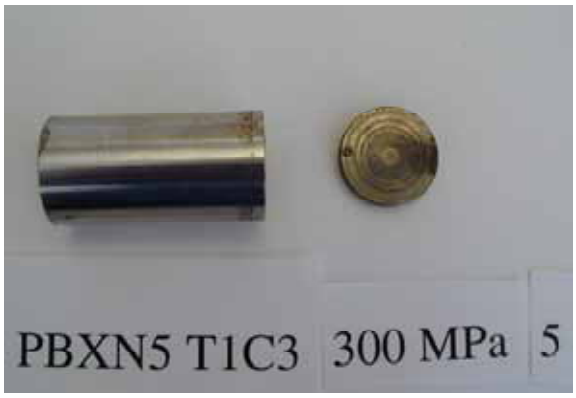

Figure 4.5: PBXN5-T1-C3. NB, the actual the position of the disk is always near the smallest diameter of the expanded tube.

The outer diameter of the steel tube was measured at three different points: At the front, in the middle and at the rear. The front is nearest to the donor charge.

Acceptor	Density	Pressure	Front	Middle	Rear	Shots
PBXN5,T1-C3	1.73g/cm^3	200MPa	27.65mm	26.23mm	25.69mm	5
PBXN5,T1-C3	1.77g/cm^3	300MPa	26.81mm	25.58mm	25.76mm	5

Tabell 4.5: PBXN5,T1-C3

Summarizing for the gap size of 70 mm(ignition pressure of 2 GPa): i) the H764 acceptor charge run into detonation. A complete detonation is achieved very soon along the tube. We believe that this also is taking place during use of the ammunition against hard targets, ii) the charge PBXN5-T2-C1 does not detonate and a closer examination of the fragments suggests that the pressure reduces along the tube, ii) the charge PBXN5-T1-C3 does not detonate and is the least shock sensitive. The deformation of the steel tube is small and the pressure clearly dismiss along the tube.

5 CONCLUSION/DISCUSSION

Three different HMX based explosives of HMX were studied in this article. We find large differences in the sensitivity of the explosives during the gap test. The sensitivity of the explosives closely follows the grain size. Small grains are less sensitive than coarser grains. Any difference in the sensitivity due to changing densities was not clearly observed.

It is of interest to compare this sensitivity for shock with the standard Bam fall hammer and friction test. These test are used for non-pressed materials. Table 5.1 show results for the Bam test. During the bam fall hammer test the 1 kg load is used for different height from 15 to 50 cm. Thus ignition at 50 cm corresponds to 5 Joule. After 5 Joule a 5 kg load is used. The different discrete energy levels are 1, 2, 3 ,4, 5, 7.5, 10, 15, 20, 25 …J.

Acceptor charge	Shock sensitivity(Gap)	Bam fall hammer test	Bam friction test	Standard Gap test (BICT)
H764	high	7.5 Joule	180 Newton	?
PBXN5-T2-C1	medium	7.5 Joule	180 Newton	24.5mm?
PBXN5-T1-C3	low	5 Joule	180 Newton	?

Table 5.1: Different sensitivities for ignition.

We thus observe that H764, which was the most sensitive during shock impact, is less sensitive during fall hammer. The shock sensitivity of pressed explosives are known to be related to

density, particle size and coating. Bowden showed that the ignition mechanism is often related to the creation of localized hot spots. These hot spots are due to compressed air pockets or due to friction between sliding surfaces in the granulate. One interesting question is of course the ignition mechanisms during our gap test experiment. The ignition pressure of 2 GPa corresponds roughly to a global temperature increase of 200 K in the acceptor charge. The decomposition temperature for HMX particles is 500 K. Thus we a very near a situation where the explosive could decompose without needed hot spots. We thus hypothesize that hot spots are only marginally related to the sensitivity for our gap test. Probably the sensitivity could be revealed by integrating the pressure versus density curve for the different pressed charges up to 2 GPa. The accumulated internal energy could then pin point the ignition threshold for the different charges during the gap test experiment. This suggests that studying the mechanical behavior together with decomposition temperature of the explosive can reveal the sensitivity during shock. Also the analyses also suggest that the threshold for ignition by adiabatic compression is the same threshold as for run up to detonation.

During gap test two scenarios is observed; i) the ignition front dismiss along the tube, ii) the charge detonates.

Our explanation is then that the decaying scenario corresponds to hot spot ignition. The tube is not confined. Thereby the pressure from the decomposing gases is too low to sustain the burning front, and the ignition dies. There can be a transition area between hot spot ignition and complete ignition. But experiments and theoretical considerations indicate that this transition regime is very narrow.

The second scenario corresponds to run up to detonation, which becomes the same threshold as for ignition due to adiabatic compression. Thus in our test the run up to detonations is started if the initial compression due to the donor is so high that the decomposition temperature of the explosive is reached. The pressure during complete ignition is so high that the hot gases sustain the detonation front. Typically the run up distance is short. Usually the diameter of the charge is so large that the temperature loss along the tube can be neglected. For further work we suggest the following studies,

i) The threshold where the charge detonate.
ii) The threshold where significant hot spot ignition starts but ignition dies away along the tube

Typically case i) is studied by bullet impact experiments. Case ii) is not studied in ordinary gap tests but most explosive charges are fully sealed and detonation can be achieved due to initial pressures far below the actual detonation pressure.

The results for the Bam fall hammer test are not so easily explained. But this time non- pressed material are used. Also the influence of hot spots could be insignificant. Thus any understanding of the ignition threshold should be looked for in the pressure density curve for the non-pressed material. It could be of interest to study the fall hammer test for pressed materials.

The BICT applies water as the filling material for the gap. The results suggest a water gap of 24.5 mm. This corresponds to a pressure of 1.5 GPa. This is near our value of 2 GPA.

Our over all conclusion is that the new gap test design is a viable way of studying the sensitivity of the explosives. Both detonation threshold and the hot spot ignition threshold can be studied. Validation experiment for computer simulations can be sanalysed.

Further studies are: 1) Integrate pressure density curve for different explosives. 2) Studying numerically the global temperature and the hot spot temperature by using Autodyn both during shock and during fall hammer.

APPENDIX A; THE MATERIAL PROPERTIES OF THE DONOR

MATERIAL NAME: PBX-9404-3

EQUATION OF STATE: JWL (Explosive)
Reference density (g/cm3) : 1.84000E+00
Parameter A (kPa) : 8.52400E+08
Parameter B (kPa) : 1.80200E+07
Parameter R1 : 4.60000E+00
Parameter R2 : 1.30000E+00
Parameter W : 3.80000E-01
C-J Detonation velocity (m/s) : 8.80000E+03
C-J Energy / unit volume (kJ/m3) : 1.02000E+07
C-J Pressure (kPa) : 3.70000E+07
Burn on compression fraction : 0.00000E+00
Pre-burn bulk modulus (kPa) : 0.00000E+00
Adiabatic constant (kPa) : 0.00000E+00
Auto. convert to Ideal Gas : No

STRENGTH MODEL: None (Hydro)
FAILURE MODEL: None
EROSION MODEL: None

MATERIAL NAME: PBX-9502, Acceptor

EQUATION OF STATE: JWL (Explosive)
Reference density (g/cm3) : 1.89500E+00
Parameter A (kPa) : 4.60300E+08
Parameter B (kPa) : 9.54400E+06
Parameter R1 : 4.00000E+00
Parameter R2 : 1.70000E+00
Parameter W : 4.80000E-01
C-J Detonation velocity (m/s) : 7.71000E+03

C-J Energy / unit volume (kJ/m3) : 7.07000E+06
C-J Pressure (kPa) : 3.02000E+07
Burn on compression fraction : 0.00000E+00
Pre-burn bulk modulus (kPa) : 0.00000E+00
Adiabatic constant (kPa) : 0.00000E+00
Auto. convert to Ideal Gas : No

STRENGTH MODEL: None (Hydro)
FAILURE MODEL: None
EROSION MODEL: Inst. Geo. Strain
Erosion Strain : 2.00000E+00

APPENDIX B; THE MATERIAL PROPERTIES OF THE ACCEPTOR

MATERIAL NAME: PBXN5-SH

EQUATION OF STATE: Compaction
Reference density (g/cm3) : 2.55000E+00
Density #1 (Pressure) (g/cm3) : 1.50000E+00
Density #2 (Pressure) (g/cm3) : 1.65700E+00
Density #3 (Pressure) (g/cm3) : 1.83000E+00
Density #4 (Pressure) (g/cm3) : 1.95000E+00
Density #5 (Pressure) (g/cm3) : 2.02900E+00
Density #6 (Pressure) (g/cm3) : 2.09500E+00
Density #7 (Pressure) (g/cm3) : 2.16000E+00
Density #8 (Pressure) (g/cm3) : 2.25900E+00
Density #9 (Pressure) (g/cm3) : 2.37700E+00
Density #10 (Pressure) (g/cm3) : 2.55000E+00
Pressure #1 (kPa) : 5.00000E+03
Pressure #2 (kPa) : 2.00000E+04
Pressure #3 (kPa) : 6.40000E+04
Pressure #4 (kPa) : 3.71000E+05
Pressure #5 (kPa) : 1.40000E+06
Pressure #6 (kPa) : 2.80000E+06
Pressure #7 (kPa) : 4.90000E+06
Pressure #8 (kPa) : 9.90000E+06
Pressure #9 (kPa) : 1.89000E+07
Pressure #10 (kPa) : 4.10000E+07
Density #1 (Soundspeed) (g/cm3) : 1.50000E+00
Density #2 (Soundspeed) (g/cm3) : 1.65700E+00
Density #3 (Soundspeed) (g/cm3) : 1.83000E+00
Density #4 (Soundspeed) (g/cm3) : 1.95000E+00
Density #5 (Soundspeed) (g/cm3) : 2.02900E+00
Density #6 (Soundspeed) (g/cm3) : 2.09500E+00

Density #7 (Soundspeed) (g/cm3) : 2.16000E+00
Density #8 (Soundspeed) (g/cm3) : 2.25900E+00
Density #9 (Soundspeed) (g/cm3) : 2.37700E+00
Density #10 (Soundspeed) (g/cm3) : 2.55000E+00
Soundspeed #1 (m/s) : 4.47000E+02
Soundspeed #2 (m/s) : 1.00000E+03
Soundspeed #3 (m/s) : 3.50000E+03
Soundspeed #4 (m/s) : 5.44000E+03
Soundspeed #5 (m/s) : 6.93000E+03
Soundspeed #6 (m/s) : 8.20000E+03
Soundspeed #7 (m/s) : 9.50000E+03
Soundspeed #8 (m/s) : 1.23000E+04
Soundspeed #9 (m/s) : 1.58100E+04
Soundspeed #10 (m/s) : 2.16200E+04

STRENGTH MODEL: M-O Granular

Pressure #1 (kPa) : 0.00000E+00
Pressure #2 (kPa) : 5.00000E+04
Pressure #3 (kPa) : 1.32000E+05
Pressure #4 (kPa) : 2.00000E+05
Pressure #5 (kPa) : 6.57000E+05
Pressure #6 (kPa) : 1.00000E+06
Pressure #7 (kPa) : 2.00000E+06
Pressure #8 (kPa) : 4.00000E+06
Pressure #9 (kPa) : 8.00000E+06
Pressure #10 (kPa) : 3.50000E+07
Yield Stress #1 (kPa) : 0.00000E+00
Yield Stress #2 (kPa) : 4.63000E+04
Yield Stress #3 (kPa) : 7.84000E+04
Yield Stress #4 (kPa) : 9.69000E+04
Yield Stress #5 (kPa) : 1.80000E+05
Yield Stress #6 (kPa) : 2.43000E+05
Yield Stress #7 (kPa) : 3.22000E+05
Yield Stress #8 (kPa) : 3.81000E+05
Yield Stress #9 (kPa) : 4.23000E+05
Yield Stress #10 (kPa) : 4.43000E+05
Density #1 (Yield Stress) (g/cm3) : 8.20000E-01
Density #2 (Yield Stress) (g/cm3) : 1.63000E+00
Density #3 (Yield Stress) (g/cm3) : 1.72000E+00
Density #4 (Yield Stress) (g/cm3) : 1.78000E+00
Density #5 (Yield Stress) (g/cm3) : 1.84000E+00
Density #6 (Yield Stress) (g/cm3) : 1.88000E+00
Density #7 (Yield Stress) (g/cm3) : 1.90200E+00
Density #8 (Yield Stress) (g/cm3) : 2.00000E+00

Density #9 (Yield Stress) (g/cm3) : 2.21000E+00
Density #10 (Yield Stress) (g/cm3) : 3.90000E+00
Yield Stress #1 (kPa) : 0.00000E+00
Yield Stress #2 (kPa) : 3.00000E+02
Yield Stress #3 (kPa) : 4.00000E+02
Yield Stress #4 (kPa) : 5.90000E+02
Yield Stress #5 (kPa) : 8.60000E+02
Yield Stress #6 (kPa) : 1.60000E+03
Yield Stress #7 (kPa) : 2.74000E+03
Yield Stress #8 (kPa) : 2.96000E+03
Yield Stress #9 (kPa) : 3.20000E+03
Yield Stress #10 (kPa) : 3.32900E+03
Density #1 (Shear Modulus) (g/cm3) : 1.50000E+00
Density #2 (Shear Modulus) (g/cm3) : 1.65700E+00
Density #3 (Shear Modulus) (g/cm3) : 1.83000E+00
Density #4 (Shear Modulus) (g/cm3) : 1.95000E+00
Density #5 (Shear Modulus) (g/cm3) : 2.02900E+00
Density #6 (Shear Modulus) (g/cm3) : 2.09500E+00
Density #7 (Shear Modulus) (g/cm3) : 2.16000E+00
Density #8 (Shear Modulus) (g/cm3) : 2.25900E+00
Density #9 (Shear Modulus) (g/cm3) : 2.37700E+00
Density #10 (Shear Modulus) (g/cm3) : 2.55000E+00
Shear Modulus #1 (kPa) : 2.04000E+05
Shear Modulus #2 (kPa) : 1.10000E+06
Shear Modulus #3 (kPa) : 1.41000E+07
Shear Modulus #4 (kPa) : 1.60000E+07
Shear Modulus #5 (kPa) : 1.81000E+07
Shear Modulus #6 (kPa) : 2.48000E+07
Shear Modulus #7 (kPa) : 3.40000E+07
Shear Modulus #8 (kPa) : 5.73000E+07
Shear Modulus #9 (kPa) : 9.75000E+07
Shear Modulus #10 (kPa) : 1.93000E+08

FAILURE MODEL: None

EROSION MODEL: None

APPENDIX C; MATERIAL PROPERTIES FOR STEEL

Steel disk

MATERIAL NAME: 12.7STEEL1

EQUATION OF STATE: Linear

Reference density (g/cm3) : 7.84000E+00
Bulk Modulus (kPa) : 1.71700E+08
Reference Temperature (K) : 2.93000E+02
Specific Heat (C.V.) (J/kgK) : 4.60000E+02

STRENGTH MODEL: Piecewise Linear

Shear Modulus (kPa) : 7.92300E+07
Yield Stress (zero strain) (kPa) : 6.45000E+05
Eff.Pl.Strain #1 : 0.00000E+00
Eff.Pl.Strain #2 : 1.00000E-01
Eff.Pl.Strain #3 : 2.00000E-01
Eff.Pl.Strain #4 : 3.00000E-01
Eff.Pl.Strain #5 : 4.00000E-01
Eff.Pl.Strain #6 : 5.00000E-01
Eff.Pl.Strain #7 : 6.00000E-01
Eff.Pl.Strain #8 : 8.00000E-01
Eff.Pl.Strain #9 : 1.00000E+00
Eff.Pl.Strain #10 : 5.00000E+00
Yield Stress #1 (kPa) : 6.45000E+05
Yield Stress #2 (kPa) : 6.90000E+05
Yield Stress #3 (kPa) : 7.25000E+05
Yield Stress #4 (kPa) : 7.70000E+05
Yield Stress #5 (kPa) : 8.00000E+05
Yield Stress #6 (kPa) : 8.35000E+05
Yield Stress #7 (kPa) : 8.65000E+05
Yield Stress #8 (kPa) : 9.15000E+05
Yield Stress #9 (kPa) : 9.60000E+05
Yield Stress #10 (kPa) : 1.77000E+06
Strain Rate Constant : 0.00000E+00
Thermal Softening Exponent : 1.00000E+02
Melting Temperature (K) : 1.77300E+03

FAILURE MODEL: Eff. Plastic Stn.

Ultimate Strain : 1.00000E-01
Crack Softening, Gf (J/m2) : 0.00000E+00
or, Kc2 (mN2/mm3): 0.00000E+00

EROSION MODEL: Inst. Geo. Strain

Erosion Strain : 2.00000E+00

Support plate:

MATERIAL NAME: 12.7STEEL2

EQUATION OF STATE: Linear

Reference density (g/cm3) : 7.84000E+00
Bulk Modulus (kPa) : 1.71700E+08
Reference Temperature (K) : 2.93000E+02
Specific Heat (C.V.) (J/kgK) : 4.60000E+02

STRENGTH MODEL: Piecewise Linear

Shear Modulus (kPa) : 7.92300E+07
Yield Stress (zero strain) (kPa) : 6.45000E+05
Eff.Pl.Strain #1 : 0.00000E+00
Eff.Pl.Strain #2 : 1.00000E-01
Eff.Pl.Strain #3 : 2.00000E-01
Eff.Pl.Strain #4 : 3.00000E-01
Eff.Pl.Strain #5 : 4.00000E-01
Eff.Pl.Strain #6 : 5.00000E-01
Eff.Pl.Strain #7 : 6.00000E-01
Eff.Pl.Strain #8 : 8.00000E-01
Eff.Pl.Strain #9 : 1.00000E+00
Eff.Pl.Strain #10 : 5.00000E+00
Yield Stress #1 (kPa) : 6.45000E+05
Yield Stress #2 (kPa) : 6.90000E+05
Yield Stress #3 (kPa) : 7.25000E+05
Yield Stress #4 (kPa) : 7.70000E+05
Yield Stress #5 (kPa) : 8.00000E+05
Yield Stress #6 (kPa) : 8.35000E+05
Yield Stress #7 (kPa) : 8.65000E+05
Yield Stress #8 (kPa) : 9.15000E+05
Yield Stress #9 (kPa) : 9.60000E+05
Yield Stress #10 (kPa) : 1.77000E+06
Strain Rate Constant : 0.00000E+00
Thermal Softening Exponent : 1.00000E+02
Melting Temperature (K) : 1.77300E+03

FAILURE MODEL: Eff. Plastic Stn.

Ultimate Strain : 1.50000E+00
Crack Softening, Gf (J/m2) : 0.00000E+00
or, Kc2 (mN2/mm3): 0.00000E+00

EROSION MODEL: Inst. Geo. Strain

Erosion Strain : 2.50000E+00

APPENDIX D; MATERIAL DATA FOR FURTHER STUDIES

MATERIAL NAME: PBXN5-ISO

EQUATION OF STATE: Compaction

Reference density (g/cm3) : 2.02900E+00
Density #1 (Pressure) (g/cm3) : 8.20000E-01
Density #2 (Pressure) (g/cm3) : 1.55000E+00
Density #3 (Pressure) (g/cm3) : 1.63000E+00
Density #4 (Pressure) (g/cm3) : 1.74000E+00
Density #5 (Pressure) (g/cm3) : 1.82000E+00
Density #6 (Pressure) (g/cm3) : 1.90200E+00
Density #7 (Pressure) (g/cm3) : 1.95500E+00
Density #8 (Pressure) (g/cm3) : 2.02900E+00
Density #9 (Pressure) (g/cm3) : 2.10000E+00
Density #10 (Pressure) (g/cm3) : 3.00000E+00
Pressure #1 (kPa) : 0.00000E+00
Pressure #2 (kPa) : 7.00000E+03
Pressure #3 (kPa) : 1.60000E+04
Pressure #4 (kPa) : 3.68000E+04
Pressure #5 (kPa) : 6.57000E+04
Pressure #6 (kPa) : 1.60000E+05
Pressure #7 (kPa) : 2.75000E+05
Pressure #8 (kPa) : 8.80000E+05
Pressure #9 (kPa) : 2.00000E+09
Pressure #10 (kPa) : 1.78000E+10
Density #1 (Soundspeed) (g/cm3) : 8.20000E-01
Density #2 (Soundspeed) (g/cm3) : 1.50000E+00
Density #3 (Soundspeed) (g/cm3) : 1.63000E+00
Density #4 (Soundspeed) (g/cm3) : 1.73000E+00
Density #5 (Soundspeed) (g/cm3) : 1.83000E+00
Density #6 (Soundspeed) (g/cm3) : 1.90000E+00
Density #7 (Soundspeed) (g/cm3) : 1.95000E+00
Density #8 (Soundspeed) (g/cm3) : 2.02900E+00
Density #9 (Soundspeed) (g/cm3) : 2.10000E+00
Density #10 (Soundspeed) (g/cm3) : 3.00000E+00
Soundspeed #1 (m/s) : 2.68000E+02
Soundspeed #2 (m/s) : 5.21000E+02
Soundspeed #3 (m/s) : 7.05000E+02
Soundspeed #4 (m/s) : 1.18800E+03
Soundspeed #5 (m/s) : 1.81000E+03
Soundspeed #6 (m/s) : 2.74000E+03
Soundspeed #7 (m/s) : 3.70000E+03
Soundspeed #8 (m/s) : 4.75000E+03
Soundspeed #9 (m/s) : 4.75000E+03
Soundspeed #10 (m/s) : 4.75000E+03

STRENGTH MODEL: M-O Granular

Pressure #1 (kPa) : 0.00000E+00
Pressure #2 (kPa) : 5.00000E+04
Pressure #3 (kPa) : 1.32000E+05
Pressure #4 (kPa) : 2.00000E+05
Pressure #5 (kPa) : 6.57000E+05

Pressure #6 (kPa) : 1.00000E+06
Pressure #7 (kPa) : 2.00000E+06
Pressure #8 (kPa) : 4.00000E+06
Pressure #9 (kPa) : 8.00000E+06
Pressure #10 (kPa) : 3.50000E+07
Yield Stress #1 (kPa) : 0.00000E+00
Yield Stress #2 (kPa) : 4.63000E+04
Yield Stress #3 (kPa) : 7.84000E+04
Yield Stress #4 (kPa) : 9.69000E+04
Yield Stress #5 (kPa) : 1.80000E+05
Yield Stress #6 (kPa) : 2.43000E+05
Yield Stress #7 (kPa) : 3.22000E+05
Yield Stress #8 (kPa) : 3.81000E+05
Yield Stress #9 (kPa) : 4.23000E+05
Yield Stress #10 (kPa) : 4.43000E+05
Density #1 (Yield Stress) (g/cm3) : 8.20000E-01
Density #2 (Yield Stress) (g/cm3) : 1.63000E+00
Density #3 (Yield Stress) (g/cm3) : 1.72000E+00
Density #4 (Yield Stress) (g/cm3) : 1.78000E+00
Density #5 (Yield Stress) (g/cm3) : 1.84000E+00
Density #6 (Yield Stress) (g/cm3) : 1.88000E+00
Density #7 (Yield Stress) (g/cm3) : 1.90200E+00
Density #8 (Yield Stress) (g/cm3) : 2.00000E+00
Density #9 (Yield Stress) (g/cm3) : 2.21000E+00
Density #10 (Yield Stress) (g/cm3) : 3.90000E+00
Yield Stress #1 (kPa) : 0.00000E+00
Yield Stress #2 (kPa) : 3.00000E+02
Yield Stress #3 (kPa) : 4.00000E+02
Yield Stress #4 (kPa) : 5.90000E+02
Yield Stress #5 (kPa) : 8.60000E+02
Yield Stress #6 (kPa) : 1.60000E+03
Yield Stress #7 (kPa) : 2.74000E+03
Yield Stress #8 (kPa) : 2.96000E+03
Yield Stress #9 (kPa) : 3.20000E+03
Yield Stress #10 (kPa) : 3.32900E+03
Density #1 (Shear Modulus) (g/cm3) : 8.20000E-01
Density #2 (Shear Modulus) (g/cm3) : 1.50000E+00
Density #3 (Shear Modulus) (g/cm3) : 1.63000E+00
Density #4 (Shear Modulus) (g/cm3) : 1.73000E+00
Density #5 (Shear Modulus) (g/cm3) : 1.83000E+00
Density #6 (Shear Modulus) (g/cm3) : 1.90000E+00
Density #7 (Shear Modulus) (g/cm3) : 1.95000E+00
Density #8 (Shear Modulus) (g/cm3) : 2.02900E+00
Density #9 (Shear Modulus) (g/cm3) : 2.10000E+00
Density #10 (Shear Modulus) (g/cm3) : 3.00000E+00
Shear Modulus #1 (kPa) : 4.21000E+04
Shear Modulus #2 (kPa) : 2.76000E+05
Shear Modulus #3 (kPa) : 5.39000E+05
Shear Modulus #4 (kPa) : 1.60000E+06
Shear Modulus #5 (kPa) : 3.75000E+06
Shear Modulus #6 (kPa) : 3.84000E+06
Shear Modulus #7 (kPa) : 5.11000E+06
Shear Modulus #8 (kPa) : 8.43000E+06

Shear Modulus #9 (kPa) : 8.65000E+06
Shear Modulus #10 (kPa) : 1.24000E+07

FAILURE MODEL: None

EROSION MODEL: None

H-764:

MATERIAL NAME: H764-AUG02

EQUATION OF STATE: Compaction

Reference density (g/cm3) : 1.89280E+00
Density #1 (Pressure) (g/cm3) : 9.20000E-01
Density #2 (Pressure) (g/cm3) : 1.50000E+00
Density #3 (Pressure) (g/cm3) : 1.60200E+00
Density #4 (Pressure) (g/cm3) : 1.70000E+00
Density #5 (Pressure) (g/cm3) : 1.77550E+00
Density #6 (Pressure) (g/cm3) : 1.83000E+00
Density #7 (Pressure) (g/cm3) : 1.86000E+00
Density #8 (Pressure) (g/cm3) : 1.89300E+00
Density #9 (Pressure) (g/cm3) : 1.96000E+00
Density #10 (Pressure) (g/cm3) : 2.12140E+00
Pressure #1 (kPa) : 0.00000E+00
Pressure #2 (kPa) : 2.40000E+03
Pressure #3 (kPa) : 1.00000E+04
Pressure #4 (kPa) : 2.40000E+04
Pressure #5 (kPa) : 5.60000E+04
Pressure #6 (kPa) : 9.20000E+04
Pressure #7 (kPa) : 1.20000E+05
Pressure #8 (kPa) : 1.63000E+05
Pressure #9 (kPa) : 3.44200E+05
Pressure #10 (kPa) : 1.66400E+06
Density #1 (Soundspeed) (g/cm3) : 9.20000E-01
Density #2 (Soundspeed) (g/cm3) : 1.50000E+00
Density #3 (Soundspeed) (g/cm3) : 1.60000E+00
Density #4 (Soundspeed) (g/cm3) : 1.75000E+00
Density #5 (Soundspeed) (g/cm3) : 1.80000E+00
Density #6 (Soundspeed) (g/cm3) : 1.83000E+00
Density #7 (Soundspeed) (g/cm3) : 1.86000E+00
Density #8 (Soundspeed) (g/cm3) : 1.89300E+00
Density #9 (Soundspeed) (g/cm3) : 2.00000E+00
Density #10 (Soundspeed) (g/cm3) : 2.20000E+00
Soundspeed #1 (m/s) : 1.04000E+02
Soundspeed #2 (m/s) : 4.47000E+02
Soundspeed #3 (m/s) : 6.37000E+02
Soundspeed #4 (m/s) : 8.52000E+02
Soundspeed #5 (m/s) : 9.60000E+02
Soundspeed #6 (m/s) : 1.28000E+03

Soundspeed #7 (m/s) : 1.65600E+03
Soundspeed #8 (m/s) : 2.05600E+03
Soundspeed #9 (m/s) : 3.59200E+03
Soundspeed #10 (m/s) : 6.15300E+03

STRENGTH MODEL: M-O Granular

Pressure #1 (kPa) : 0.00000E+00
Pressure #2 (kPa) : 5.00000E+04
Pressure #3 (kPa) : 1.32000E+05
Pressure #4 (kPa) : 2.00000E+05
Pressure #5 (kPa) : 3.53000E+05
Pressure #6 (kPa) : 5.21000E+05
Pressure #7 (kPa) : 6.57000E+05
Pressure #8 (kPa) : 7.44000E+05
Pressure #9 (kPa) : 8.67000E+05
Pressure #10 (kPa) : 1.00000E+06
Yield Stress #1 (kPa) : 0.00000E+00
Yield Stress #2 (kPa) : 5.38000E+04
Yield Stress #3 (kPa) : 7.75000E+04
Yield Stress #4 (kPa) : 9.49000E+04
Yield Stress #5 (kPa) : 1.29000E+05
Yield Stress #6 (kPa) : 1.60600E+05
Yield Stress #7 (kPa) : 1.85100E+05
Yield Stress #8 (kPa) : 1.97800E+05
Yield Stress #9 (kPa) : 2.08100E+05
Yield Stress #10 (kPa) : 2.18400E+05
Density #1 (Yield Stress) (g/cm3) : 9.20000E-01
Density #2 (Yield Stress) (g/cm3) : 1.50000E+00
Density #3 (Yield Stress) (g/cm3) : 1.69500E+00
Density #4 (Yield Stress) (g/cm3) : 1.75000E+00
Density #5 (Yield Stress) (g/cm3) : 1.80000E+00
Density #6 (Yield Stress) (g/cm3) : 1.83000E+00
Density #7 (Yield Stress) (g/cm3) : 1.86000E+00
Density #8 (Yield Stress) (g/cm3) : 1.87000E+00
Density #9 (Yield Stress) (g/cm3) : 1.89300E+00
Density #10 (Yield Stress) (g/cm3) : 2.20000E+00
Yield Stress #1 (kPa) : 0.00000E+00
Yield Stress #2 (kPa) : 2.80000E+01
Yield Stress #3 (kPa) : 2.06000E+03
Yield Stress #4 (kPa) : 2.66000E+03
Yield Stress #5 (kPa) : 3.23000E+03
Yield Stress #6 (kPa) : 3.61000E+03
Yield Stress #7 (kPa) : 3.99000E+03
Yield Stress #8 (kPa) : 4.21000E+03
Yield Stress #9 (kPa) : 6.27000E+03
Yield Stress #10 (kPa) : 6.27000E+03
Density #1 (Shear Modulus) (g/cm3) : 9.20000E-01
Density #2 (Shear Modulus) (g/cm3) : 1.50000E+00
Density #3 (Shear Modulus) (g/cm3) : 1.60000E+00
Density #4 (Shear Modulus) (g/cm3) : 1.75000E+00
Density #5 (Shear Modulus) (g/cm3) : 1.80000E+00

Density #6 (Shear Modulus) (g/cm3) : 1.83000E+00
Density #7 (Shear Modulus) (g/cm3) : 1.86000E+00
Density #8 (Shear Modulus) (g/cm3) : 1.89300E+00
Density #9 (Shear Modulus) (g/cm3) : 2.00000E+00
Density #10 (Shear Modulus) (g/cm3) : 2.20000E+00
Shear Modulus #1 (kPa) : 7.19000E+03
Shear Modulus #2 (kPa) : 2.07465E+05
Shear Modulus #3 (kPa) : 4.35808E+05
Shear Modulus #4 (kPa) : 7.98871E+05
Shear Modulus #5 (kPa) : 1.00078E+06
Shear Modulus #6 (kPa) : 1.62992E+06
Shear Modulus #7 (kPa) : 2.40833E+06
Shear Modulus #8 (kPa) : 3.27273E+06
Shear Modulus #9 (kPa) : 5.88551E+06
Shear Modulus #10 (kPa) : 1.78500E+07

FAILURE MODEL: Hydro

Hydro Tensile limit (PMIN) (kPa) : -5.00000E+03
Reheal : Yes
Crack Softening, Gf (J/m2) : 0.00000E+00
or, Kc2 (mN2/mm3): 0.00000E+00

EROSION MODEL: Inst. Geo. Strain

Erosion Strain : 2.00000E+00